GEOPHYSICAL RESEARCH LETTERS, VOL. 26, NO. 22, PAGES 3345-3348, NOVEMBER 15, 1999

Gradient drift instability in high latitude plasma patches: ion inertial effects

N. A. Gondarenko and P. N. Guzdar
Institute for Plasma Research, University of Maryland, College Park

Abstract. Nonlinear simulations of the gradient drift instability with inertial effects for the high latitude plasma patches demonstrate that the initial cross-field elongated structures, driven by the gradient drift instability, are unstable to the Kelvin-Helmholtz instability and to the generation of sheared flows. The shear flow develops on the scale-length of the irregularities. Both these processes arise from the nonlinear inertial term. The computed density and velocity fluctuation levels are of the order of the observed values. The combined effect of parallel dynamics as well as secondary instabilities prevent the patch from disintegrating for hours.

Introduction

The high latitude ionospheric plasma has irregularities which range from meters to hundreds of kilometers of spatial scale and from minutes to hours of temporal scale [*Tsunoda,* 1988; *Crowley,* 1996; *Basu and Valladares,* 1999]. The large or macro-scales (hundreds of kilometers) have been characterized as "patches" (in the polar cap), or "blobs" (at auroral latitudes) [*Weber et al.,* 1984, 1986; *Basu et al.,* 1990; *Basu et al.,* 1994]. The mesoscales in the range of 0.1 km to tens of kilometers, may be due to a plasma instabilities. Observations [*Weber et al.,* 1986; *Basu et al.,* 1994] and modeling studies [*Sojka et al.,* 1993] indicate that the patches convect to long distances, $\sim$ 3000 km [*Weber et al.,* 1986] and for long periods of time (hours) while retaining their distinct identity. The irregularities are observed in association with these patches throughout the polar cap region [*Weber et al.,* 1984, and 1986; *Tsunoda,* 1988; *Basu et al.,* 1990; *Basu et al.,* 1994], occasionally being more intense on the trailing edge than on the leading edge [*Weber et al.,* 1984].

In an earlier paper, three-dimensional (3-D) nonlinear simulations were presented for the collisional gradient-drift instability (GDI) [*Guzdar et al.,* 1998] to model the mesoscale structures. The basic structuring occurred transverse to the direction of the magnetic field and to the direction of the ambient density gradient in long elongated "fingers". The inclusion of dynamics along the field line was responsible for slowing down the structuring process due to the stabilizing influence of parallel electric fields [*Chaturvedi and Huba,* 1987]. Here we demonstrate that in the presence of the nonlinear ion inertial effects, these structures are unstable to secondary instabilities. The highly elongated vortices associated with fingers are unstable to the Kelvin-Helmholtz instability, which breaks up the elongated vortices into smaller vortices. These small scale vortices can further undergo a second instability which generates shear flow transverse to the magnetic field and to the direction of the ambient density gradient. Thus the final nonlinear state consists of density and potential fluctuation embedded in multiple shear layers on the scale-size of the irregularities.

Paper number 1999GL003647.
0094-8276/99/1999GL003647$05.00

Basic Equations

The starting equations are 3-D generalization of the two-dimensional (2-D) equations used by *Mitchell et al.* [1985]. For a plasma patch in a uniform magnetic field along the z direction, they are the electron continuity equation and the 'vorticity' equation,

$$\frac{\partial n}{\partial t} - \frac{c}{B_0}\nabla\phi \times \hat{z}\cdot\nabla n + \frac{\partial}{\partial z}\frac{1}{e\eta_e}\left[\frac{\partial \phi}{\partial z} - \frac{T_e}{ne}\frac{\partial n}{\partial z}\right] = 0 \quad (1)$$

$$\frac{c}{B_0\Omega_i}\nabla_\perp \cdot \left[n\left(\frac{\partial}{\partial t} - \frac{c}{B_0}\nabla\phi\times\hat{z}\cdot\nabla + \nu_{in}\right)\nabla_\perp\phi\right] + \frac{\nu_{in}}{\Omega_i}\left(\hat{z}\times\vec{V_n}\right)\cdot\nabla n + \frac{\partial}{\partial z}\frac{1}{e\eta_e}\left[\frac{\partial\phi}{\partial z} - \frac{T_e}{en}\frac{\partial n}{\partial z}\right] = 0 \quad (2)$$

where the symbols have their standard meaning: n, c, e, ϕ, T, $\vec{V_n}$, refer to plasma density, velocity of light, electronic charge, electrostatic potential, temperature in energy units, and the neutral-wind velocity respectively. $\eta_e = m_e\nu_e/ne^2$, and $\Omega_a = e_aB_0/m_ac$ ($e_a = \pm e$) is the cyclotron frequency of species $\alpha(e,i)$. $\nu_e = \nu_{ei} + \nu_{en}$ is the sum of the electron-ion and electron-neutral collision frequencies, and ν_{in} is the ion-neutral collision frequency. In equations (2), the new terms compared to our earlier work [*Guzdar et al.,* 1998], are the ion inertia effects, which are the first two terms. In previous work on high latitude interchange instabilities by *Keskinen and Huba* [1990], the effects of parallel dynamics was modeled in 2-D by introducing a wavelength-dependent frequency in the vorticity equation which preferentially stabilized the long wavelengths. Here we solve the complete 3-D system of equations.

The basic geometry for the high latitude plasma patch is the following. The Earth's field lines are vertical and aligned with the z axis. The $-x$ axis points anti-sunward, which is also the direction of convection of the patch and the y axis is orthogonal to the x and z directions. Thus the right side of the patch with the negative density gradient is the trailing edge. A set of typical parameters for the high-latitude ionosphere is $T_e \sim T_i \sim 0.1\ eV$; $L_n \sim 50\ km$; $V_0 \sim 500\ m/s$; $\gamma_0 \sim V_0/L_n \sim 10^{-2}\ s^{-1}$; $\Omega_e \sim 10^7\ rad/s$; $\Omega_i \sim 10^2\ rad/s$; $\nu_{ei} \sim 10^3\ s^{-1}$; $\nu_{in} \sim 0.1\ s^{-1}$. Here V_0 is the net drift velocity of the patch which is a combination of the electric-field and the neutral-wind drift.

Numerical Results

The normalizations for the dependent and independent variables are: $t \rightarrow t(V_0/L_n)$, $\phi \rightarrow \phi(c/L_0V_0B_0)$, $n \rightarrow n/N_0$, $z \rightarrow z/L_z$, $x \rightarrow x/L_0$, and, where L_0 is a characteristic scale-length transverse to the direction of the magnetic field, to be defined later, L_z is a characteristic scale-length along the direction of the magnetic field, and N_0 is the undisturbed ambient density of the background ionosphere away from patch/blob (independent of x). These normalizations give rise to two dimensionless parameter,

$$\beta = \frac{\Omega_e\Omega_i}{\nu_e\nu_{in}}\frac{L_0^2}{L_z^2} \tag{3}$$

$$\nu = \nu_{in}L_n/V_0 \tag{4}$$

The size of the box in the x and z directions is 4π and in the y is $\pi/2$. The reduced size in the y direction is motivated by the need for resolution of the small scale fingers and for the secondary KH instabilities. Also, to allow for more resolution in the x direction we consider

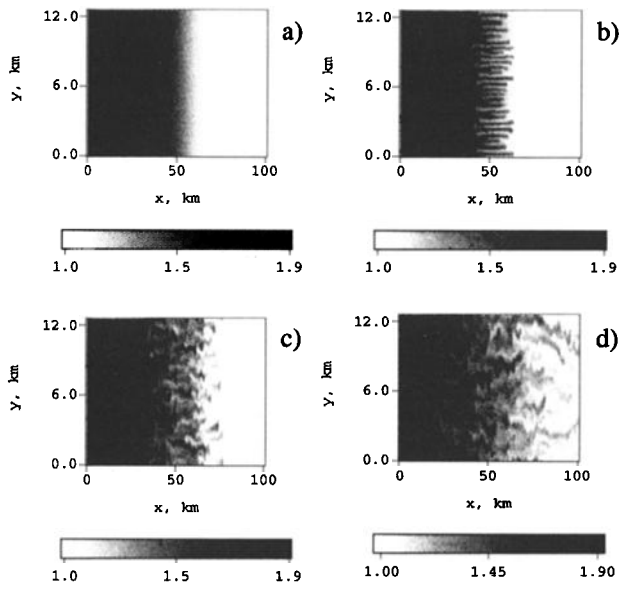

Figure 1. Density contours in the xy plane at $z = L_z/4$ for (a) t=4, (b) t=8, (c) t=14, and (d) t=36.5. The parameters used are β=2000 and ν=10.

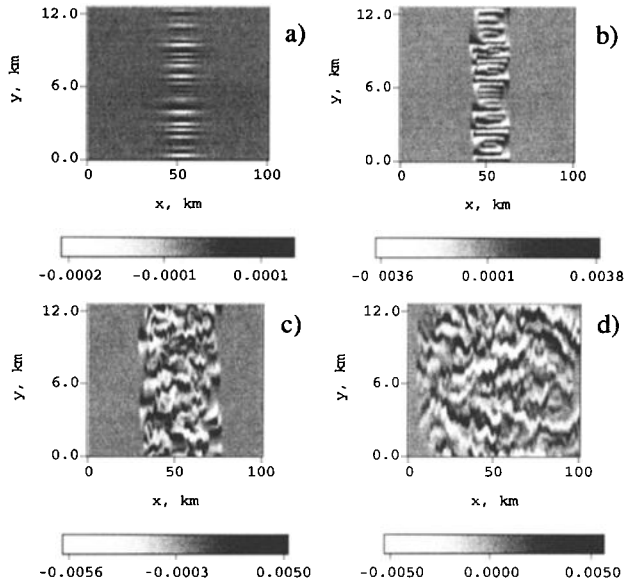

Figure 2. Potential contours in the xy plane at $z = L_z/4$ for (a) t=4, (b) t=8, (c) t=14, and (d) t=36.5. The parameters used are β=2000 and ν=10.

half the patch. For a patch size of about 200 km, for half the patch, $4\pi L_0 = 100$ km. This means that $L_0 = 8$ km. Using the values for the collision and cyclotron frequencies given above, we choose $\beta = 2000$. For this choice of the parameter β, the scale-length $L_z = 560$ km. The typical value of $\nu = 10$. The density profile in x is a tanh function to model a localized patch and for the z dependence we use the Chapman function. The peak density is twice the background density. The profiles are the same as those used in our earlier work as are the boundary conditions [*Guzdar et al.*, 1998].

We initialize the perturbed density as a superposition of $m = 1, 70$ sine modes in the y direction with random phases. The amplitude of each of the harmonics is assumed to be inversely proportional to the transverse wavenumber of the mode. The variation in the x direction is $\sin(\pi x/L_x)$ for each of the modes. We do not introduce any variations for the initial perturbations in the z direction. The number of grid points used in these simluations are $N_x = 258$, $N_y = 129$ and $N_z = 49$. The initial amplitude for each of the modes was assumed to be 0.001. With the currently available computational resources the physical size of the simulation box in the x direction is 100 km and in the y direction it is 12.5 km.

In Figures 1a-1d we show the evolution of the density in the xy plane near the peak of the Chapman function density profile in z, at four different instants of time, t=4, 8, 14, and 36.5. In Figures 2a-2d we display the potential contours for the same cut in the xy plane for the same instants of time as the density in Figure 1. At t=4, the instability which grows from the initial perturbations has not grown significantly so as to drastically modify the initial density profile. As a consequence the

density contours, as seen in Figure 1a, are almost identical to the initial profile except for some minor perturbations on the steepest part of the density gradient. The potential contours at the same instant of time in Figure 2a show a strong localization in the x direction on the steepest part of the density gradient as is to be expected. The high mode numbers in the y direction grow preferentially since the low mode numbers are strongly stabilized by the parallel dynamics.

As time progresses, at t=8 the modes have grown to large amplitude as seen in Figure 1b and the small scale fingers have grown on the trailing edge protruding into the lower density region. We also observe secondary bifurcations of the fingers in which an original finger bifurcates into two fingers. The potential structures are long elongated vortices with an extent in the x direction exceeding the size in the y direction (Figure 2b). At this stage in the development of the instability the basic characteristics are very similar to that observed in our earlier work [*Guzdar et al.*, 1998] without the inertia effects. But we must also remind the reader that the parameters used in these simulations are realistic compared to our earlier work where our main focus was demonstrating the stabilizing influence of the parallel dynamics.

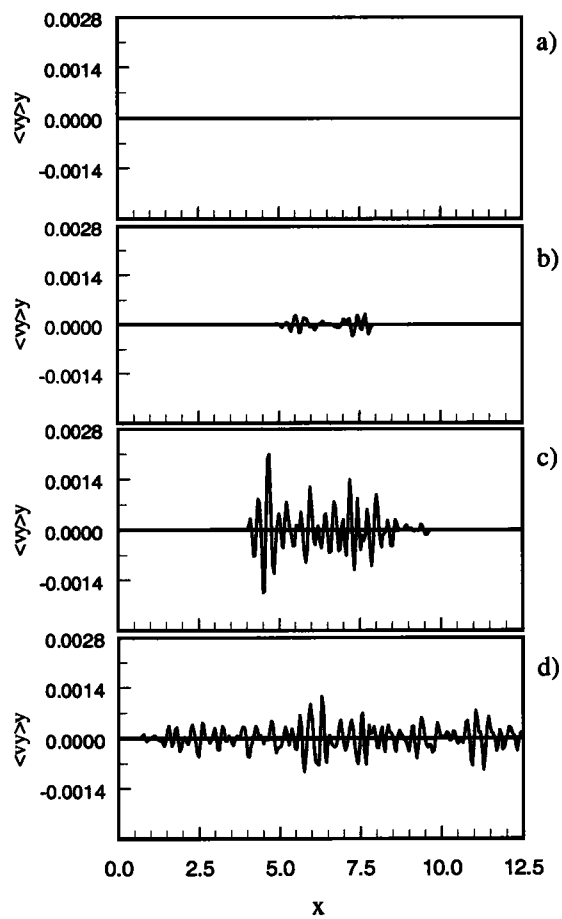

Figure 3. average v_y velocity as a function of x at(a) t=4, (b) t=8, (c) t=14, and (d) t=36.5. The parameters used are β=2000 and ν=10.

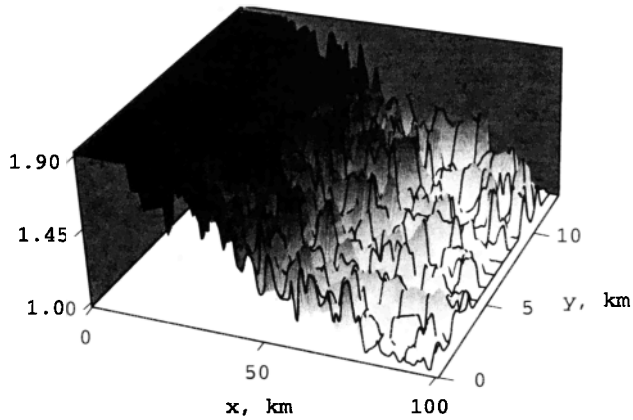

Figure 4. Density in the xy plane at $z = L_z/4$ for t=36.5. The parameters used are β=2000 and ν=10.

These highly elongated vortices are like shear flows and as a consequence can become unstable to the Kelvin-Helmholtz instability. This is clearly seen in Figures 1c and 2c. The original fingers in the density, which were extended in the x direction have now developed a wavy structure. In fact, there is distinct tilt of these fingers in the y direction. This is seen both in the density contours Figure 1c and potential contours Figure 2c. Such feature have been observed in the structuring of patches [*Pedersen*, 1998]. Finally, in Figures 1d and 2d the density and potential contours at t=36.5 are displayed. The instability has progressed all the way into the bulk of the patch. Again we remind the reader that for better resolution we have considered only one half of the patch. The secondary structuring and tilting of the fingers is clearly seen. Another interesting feature of the structuring is that at late times, the scale-length in y is larger than that at t=8. This is a consequence of the inverse cascade nature of the nonlinear inertial terms included in the present work.

One of the most interesting aspects of the simulations is the generation of shear flow transverse to the direction of propagation. Averaging the vorticity equation over y and z and performing an integral over x we can derive the following equation for the average momentum in y

$$\left(\frac{\partial}{\partial t} + \nu_{in}\right)\langle p_y\rangle - \frac{c}{B_0}\frac{\partial}{\partial x}\left\langle \frac{\partial \tilde{\phi}}{\partial y}\tilde{p}_y \right\rangle = 0 \qquad (5)$$

where $p_y = nv_y$ is the momentum in the y direction and the angular bracket $\langle\rangle$ denotes the averaging over y and z. Equation (5) shows that the fluctuating potential $\tilde{\phi}$ and the momentum $\tilde{p_y}$ can drive average flows $\langle p_y\rangle$. The driving term is referred to as the Reynolds stress. This driving term arises from the nonlinear inertial term. The ion-neutral collision damps the flow. Since at $t = 0$ we had no net momentum in the y direction, this equation shows that no net momentum should be generated at later time. This however does not preclude generation of regions of shear flows which when

averaged over x produce no net momentum in the y direction. Thus based on the constraint of no net momentum we can at best expect to see multiple shear layers or zonal flows. In Figures 3a-3d are shown the time development of the shear velocity in the y direction at t= 4, 8, 14, and 36.5, respectively. What is observed is that as the instability spreads in the x direction multiple shear layers are produced. The production of the shear layers also inhibits the rapid spreading of the irregularities in the direction of the gradient since it convects the density transverse to the x direction. Thus the combined effect of three-dimensional GDI and the inertia dominated nonlinear development contribute to the robustness of the patch, and the characteristics of the structuring are in better agreement with observations [*Kivanç and Heelis*, 1998; 1999] compared to our earlier work. Detailed comparisons between the observations and simulations need to be undertaken and are currently being done. The fluctuation level of the density is of the order of $5-10\%$ and the potential fluctuations are in the range of $0.1-1.0$ V. The self-consistent shear flows and velocity fluctuations are of the order of $0.1-1$ m/s. If we were to assume that our equilibrium flow of 500 m/s was mostly due to equilibrium electric fields this would imply that the fluctuating electric field is $0.4-4$ % of the equilibrium field. This is about 25 % - 40 % of the density fluctuations in reasonable agreement with observations [*Kivanç and Heelis*, 1999]. We have varied the parameter ν from 10 to 1000 and find that the system evolves from the inertia dominated regime presented in this paper to the collision dominated regime of our earlier work where the fluctuation in the electric field is much less compared to the density fluctuations. Also the generation of shear flow is weaker for the more collisional case.

Finally, in Figure 4 we show the density surface at t=36.5. What is clear from this plot is that the patch retains a certain robustness visually even with the instability permeating through the body of the patch. This is because the short scale-length instabilities dominate the structuring process. The parallel dynamics suppresses the longer wavelength instabilities for the gradient drift modes. Then the secondary instability due KH instability tries to isotropize the irregularities in the plane perpendicular to the magnetic field, and finally the shear flow generated by the Reynolds stress further inhibits the rapid spreading of irregularities. Thus with the combined effect of three-dimensional dynamics and inertial effects, the GDI is less destructive than that observed in earlier 2-D simulations [*Mitchell et al.*, 1985]. Also the computed levels of density and velocity or electric field fluctuations are in reasonable agreement with observations. Future work will focus on more detailed comparisons between observations and simulations.

Acknowledgments. We acknowledge useful discussions with Drs. Sunanda Basu, Shantimay Basu, Rod Heelis, Todd Pedersen and Jan Sojka. This research was supported by the NSF under grant ATM-9813861.

References

Basu, Su., et al., Plasma structuring by the gradient drift instability at high latitudes and comparison with velocity shear driven processes, *J. Geophys. Res.*, 95, 7799, 1990.

Basu, S., et al., Irregularity structures in the cusp/cleft and polar cap regions, *Radio Sci.*, 29, 195, 1994.

Basu, S., et al., Macroscale modeling and mesoscale observations of plasma density structures in the polar cap, *Geophys. Res. Lett.*, 22, 881, 1995.

Basu, Su., and Cesar Valladares, Global aspects of plasma structures, *J. Atmos. Sol-Terr. Phys.*, 61, 127, 1999.

Chaturvedi, P. K., and J. D. Huba, The interchange instability in high latitude plasma blobs, *J. Geophys. Res.*, 92, 3357, 1987.

Crowley, G., Critical Review on Ionospheric Patches and Blobs, *The Review of Radio Sci.*, Oxford University Press, 1, 1996.

Guzdar, P. N., et al., Three-dimensional nonlinear simulations of the gradient drift instability in the high latitude ionosphere, *Radio Sci.*, 33, 1901, 1998.

Keskinen, M. J., and J. D. Huba, Nonlinear evolution of high latitude ionospheric interchange instabilities with scale-size-dependent magnetospheric coupling, *J. Geophys. Res.*, 95, 15157, 1990.

Kivanç, Ö , and R. A. Heelis, Spatial distribution of ionospheric plasma and field structures in the high latitude F region, *J. Geophys. Res.*, 102, 6955, 1998.

Kivanç, Ö , and R. A. Heelis, Structures in ionospheric number density and and velocity associated with polar cap ionization patches, *J. Geophys. Res.*, 103, 307, 1999.

Mitchell, H., et al., A simulation of high-latitude F-layer instabilities in the presence of magnetospheric-ionospheric coupling, *Geophys. Res. Lett.*, 12, 283, 1985.

Pedersen, T., Incoherent radar observations of polar cap F-Layer ionization patches, *Ph. D. thesis*, Utah State University, 1998.

Sojka, J. J., et al., Modeling polar cap F-region patches using time varying convection, *Geophys. Res. Lett.*, 20, 1783, 1993.

Tsunoda, R. T., High-latitude F region irregularities: A review and synthesis, *Rev. Geophys.*, 26, 719, 1988.

Weber, E. J., et al., F layer ionization patches in the polar cap, *J. Geophys. Res.*, 89, 1683, 1984.

Weber, E. J., et al., Polar cap F patches: Structure and dynamics, *J. Geophys. Res.*, 91, 12121, 1986.

N. A. Gondarenko and P. N. Guzdar, Institute for Plasma Research, University of Maryland, College Park, MD 20742. (e-mail:natalia@ipr.umd.edu; guzdar@ipr.umd.edu)

(Received July 23, 1999; revised September 24, 1999; accepted September 30, 1999.)